# THE ITEA ($M_s$ ~ 5.9) EARTHQUAKE OF NOVEMBER 18, 1992. CHARACTERISTICS OF THE MAIN SHOCK INFERRED FROM BODY WAVE AND GROUND DISPLACEMENT ANALYSIS

Briole,P.*, Deschamps,A.**, Lyon-Caen,H.*, Papazissi,K.*** and Martinod,J.****

* Institut de Physique du Globe, Département de Sismologie, 4 Place Jussieu, 75252 Paris Cedex 05, France.
** Institut de Géodynamique, CNRS - Université de Nice-Sophia Antipolis, Avenue A. Einstein, 06560 Valbonne, France.
*** Laboratory of Higher Geodesy, Department of Surveying Engineering, National Technical University of Athens, 15780 Zographos, Athens, Greece.
**** LGIT-IRIGM, Observatoire de Grenoble, BP 53X, 38041 Grenoble Cedex, France.

## A B S T R A C T

Immediately after the Itea earthquake ($M_s$ ~ 5.9) of 18/11/1992 (Gulf of Corinth), we re-surveyed a part of a geodetic (GPS) network established in 1991. Our data show that between September 1991 and December 1992, points S and V located in the northern coast of the Gulf were displaced to the north 23 and 19 mm respectively with respect to point X located on the southern coast. These values represent the sum of some amount of continuous displacement over the 14 month period and the coseismic displacement associated with the earthquake. In this paper, we first present the characteristics of the earthquake deduced from the body wave analysis. Starting with this information, we estimate the ground displacement expected from the earthquake in both cases allowed by the focal mechanism: north-dipping fault plane or south-dipping fault plane. The value of the seismic moment limits the predicted displacement at 18 mm and 12 mm respectively in the two cases of orientation of the fault. Although the coseismic displacements are very small and close to the error bars, our results indicate that a fault plane dipping south, antithetic to the main active faults, is the most probable hypothesis. This conclusion is in good agreement with the location of the damages reported after the earthquake.

# Ο ΣΕΙΣΜΟΣ ΤΗΣ ΙΤΕΑΣ ($M_s$~5.9) ΤΗΣ 18ης ΝΟΕΜΒΡΙΟΥ 1992: ΧΑΡΑΚΤΗΡΙΣΤΙΚΑ ΤΟΥ ΚΥΡΙΟΥ ΣΕΙΣΜΟΥ ΑΠΟ ΤΗΝ ΑΝΑΛΥΣΗ ΤΩΝ ΚΥΜΑΤΩΝ ΧΩΡΟΥ ΚΑΙ ΤΗΣ ΕΔΑΦΙΚΗΣ ΠΑΡΑΜΟΡΦΩΣΗΣ

Briole,P., Deschamps,A., Lyon-Caen,H., Papazissi,K., and Martinod,J.

## Π Ε Ρ Ι Λ Η Ψ Η

Αμέσως μετά το σειομό της Ιτέας ($M_s$ ~ 5.9) της 18ης

Νοεμβρίου 1992 (Κόλπος της Κορίνθου), ξαναμετρήθηκε ένα τμήμα του γαιωδετικού δικτύου (GPS) που εγκαταστάθηκε το 1991. Τα δεδομένα δείχνουν οτι μεταξύ του Σεπτεμβρίου 1991 και του Δεκεμβρίου 1992, τα σημεία S και V που βρίσκονται στη βόρεια ακτή του κόλπου μετατοπίσθηκαν προς το βορρά κατά 23 και 19 mm, αντίστοιχα σε σχέση με το σημείο X που βρίσκεται στην νότια ακτή. Αυτές οι τιμές αντιπροσωπεύουν το άθροισμα ενός ποσού συνεχούς μετατόπισης κατά το διάστημα των 14 μηνών καθώς και την μετατόπιση που οφείλεται στο σεισμό. Στη εργασία αυτή, παρουσιάζουμε πρώτα τα χαρακτηριστικά του σεισμού όπως προκύπτουν απο τη ανάλυση των κυμάτων χώρου. Με βάση τα στοιχεία αυτά υπολογίσαμε την εδαφική μετατόπιση που αναμένεται για δύο περιπτώσεις: για ένα ρήγμα που κλίνει προς το βορρά και για ένα ρήγμα που κλίνει προς το νότο. Η τιμή της σεισμικής ροπής περιορίζει την προβλεπόμενη μετατόπιση σε 18mm και 12mm αντίστοιχα για τις δυο περιπτώσεις προσανατολισμού του ρήγματος. Αν και οι μετατοπίσεις κατά την διάρκεια του σεισμού είναι πολυ μικρές και κοντά στα όρια του σφάλματος, τα αποτελέσματα δείχνουν ότι ένα ρήγμα το οποίο κλίνει προς το νότο, και είναι αντιθετικό με τα κύρια ενεργά ρήγματα της περιοχής, είναι το πιο πιθανό. Αυτό το συμπέρασμα είναι σε καλή συμφωνία με την κατανομή των βλαβών που προήρθαν απο το σεισμό.

## INTRODUCTION

The Gulf of Corinth is one of the most seismically active areas of Greece. Since ancient time, large earthquakes are known to have occurred around the Gulf, however only the 1981 earthquakes near Corinth have been studied in detail (Jackson et al., 1982; King et al., 1985), giving information on the deformation mechanism of the Gulf. The structure of this graben is asymmetric, the main active normal faults being located on the southern side of the Gulf and dipping north (figure 1). The extension rate across the Gulf has been estimated to be 1-1.5 cm/yr (Billiris et al., 1991; Rigo et al., (1), this issue). The $M_s$ = 5.9 Itea earthquake of November 18, 1992 occurred in the central part of the Gulf close to the epicenters of the 6/7/1965 ($m_b$ = 5.8, Ambraseys and Jackson, 1990) and 8/4/1970 ($m_b$ = 5.8, Liotier, 1989) events (figure 1). Although the location of the main shock is not very precisely known due to the lack of a close station, both the USGS and Thessaloniki Observatory locate the event off shore close to the northern border of the Gulf (figure 1), just in front of one of the most prominent active faults, the Xylokastro normal fault. The fact that no surface faulting has been observed, that the event was essentially felt in the northern side of the Gulf where all the damage has been reported (in particular Galaxidi and Itea) and that a small tsunami wave (a few decimeters high) has been observed in the Galaxidi harbour, point also to a location off shore but close to the northern border.

In this paper we present the results of body wave inversion to retrieve the fault plane parameters and of deformation studies for the main shock, taking advantage of microseismic and geodetic observations obtained through a multidisciplinary study of the Patras-Aigion area (Rigo et al., (1-2), this issue). We use this

information to present a model of faulting for this earthquake.

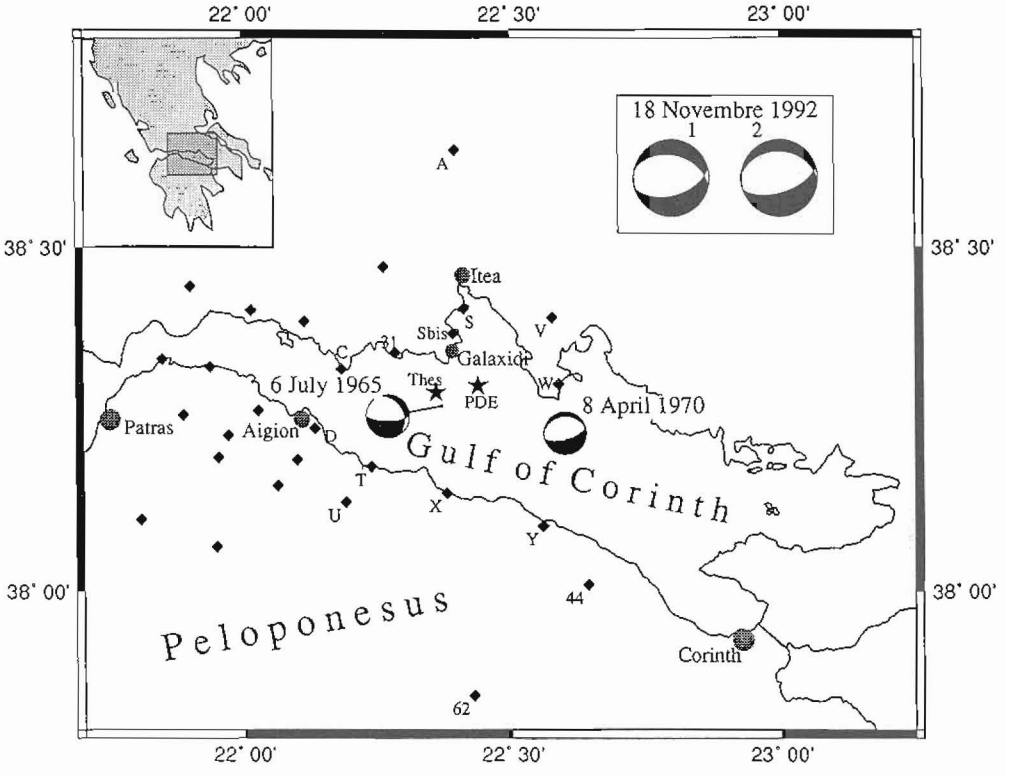


Fig.1. Regional map of the Gulf of Corinth. The two larger earthquakes that occured in the region during the last 30 years are reported in place with their focal mechanism (Ambraseys and Jackson, 1990; Liotier, 1989). Triangles are the 18th November 1992 event's epicenter determinations from USGS and Thessaloniki Observatory. Focal mechanisms in the upper right corner are 1) Harvard moment tensor solution, 2) body wave solution from this paper. Small full diamonds represent the geodetic network measured in 1991.

## FOCAL MECHANISM AND SEISMIC MOMENT

We inverted ground displacement obtained from teleseismic records of worldwide broad-band stations to determine the focal mechanism, the centroid depth and the seismic moment of the event using McCaffrey and Abers's (1988) PC version of Nabelek's (1984) inversion program. Broad band records allow to constrain well the shallow depth due to the presence of high frequencies, the seismic moment and fault plane parameters being better constrained by the low frequencies.

We retrieved seismograms from the IRIS-DMC and GEOSCOPE centers and selected P waves between 30° and 85° and SH waves between 40° and 70°. At these distances body waves travel mostly in the lower mantle and synthetic seismograms can easily be computed.

We thus selected 20 P and 11 SH waves. Most of them belong to the Russian and Chinese network since a lot of stations recording on local trigerring did not record the event which was not very large or recorded only the S wave. At some other stations, the intermediate period noise was quite large and did not allow to recover the ground displacement in the usefull frequency range (i.e. SUR). The azimuthal coverage is thus rather poor with only two P waves (BNG: D = 34°, f = 187° ; MBO: D = 42°, f = 246°) and one S wave (MBO) in the southern part of the focal sphere.

The inversion was performed using displacement waveforms sampled at 4 and 2 points per seconds for P and S waves respectively. 10 parameters are determined (strike, dip, slip, centroid depth and the amplitudes of 6 1sec long triangles describing the source time function). We used the velocity model obtained by Rigo et al. (2) (this issue) from a microseismicity study in the area, adding a 0.5 km thick layer of water (table 1) since most probably, as discussed in the introduction, the epicenter was located in the Gulf of Corinth, south of Galaxidi and not on shore.

Table 1. Velocity model used in waveform modelling.

| h (km) | vp (km/sec) | vs (km/sec) | r (kg/dm3) |
|---|---|---|---|
| < 0.5 | 1.5 | 0. | 1.03 |
| 0.5 - 4.5 | 4.9 | 2.7 | 2.6 |
| > 4.5 | 5.4 | 3 | 2.7 |

The final solution is presented in figure 2. The centroid depth (7.41 km) is well constrained and is compatible with the depth distribution of microearthquakes recorded in 1991 (Rigo et al. (2), this issue) as well as with the observation of a tsunami in the Galaxidi harbour during the earthquake. Due to the poor azimuthal distribution of data, the fault parameters are less well constrained, in particular the slip. Key observations are the clear nodal dilatational P wave at BNG and the SH wave recorded at MBO. The obtained solution (strike= 80±10°, dip=60±3°, slip= -95±10°) represents almost pure normal faulting on an ENE striking plane and is similar to the fault plane solution of the 1965 Eratini earthquake (Ambraseys and Jackson, 1990) and that of 1970 (Liotier, 1989). The seismic moment ($5.2 \cdot 10^{17}$ Nm) is clearly released in two different sub-events represented on the source time function by two lobes, both of them having almost the same amplitude and the same duration of 2 sec. However the relative position of these two sub-events cannot be resolved by this data set. In the following, we suppose that all the displacement and moment release took place on the

same fault plane. The relation between the seismic moment Mo, the fault surface S and slip d ($M_o$= mSd) implies some bound on the amplitude of slip and on the surface of the fault. We use these constraints to interpret the geodetic observations discussed below.

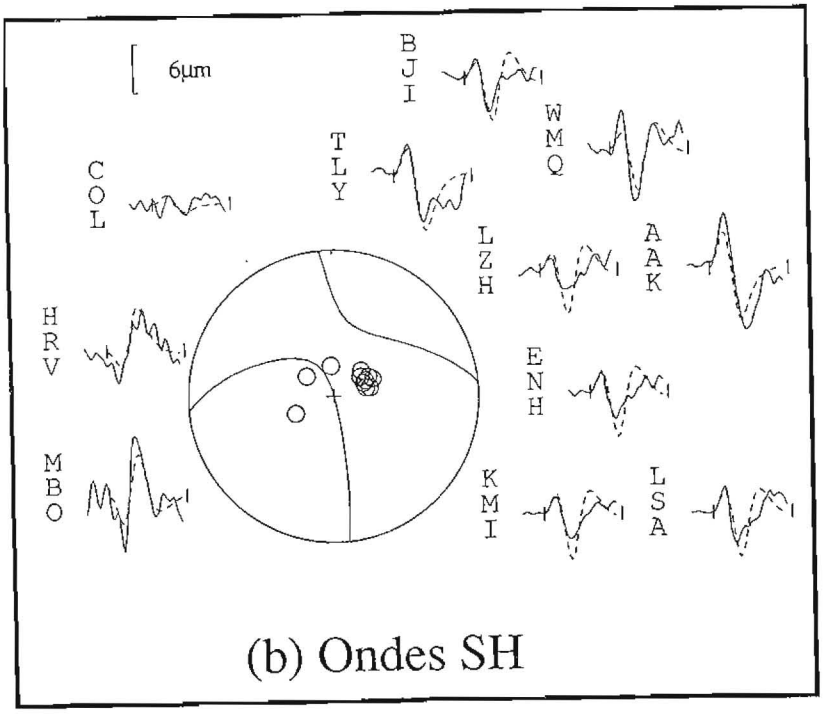


Fig.2. Body wave modelling : P (a) and SH (b) displacement waveforms are presented with the focal sphere. Continuous lines are observed and dashed lines are synthetic seismograms corresponding to the preferred solution (focal depth 7.4 km, dip = 60°, strike = 80°, slip = -95°). All amplitudes are normalised and directly comparable. The source time function on the left shows the double pulse clearly observed on almost all the data.

## GPS DATA ANALYSIS

GPS observations were performed immediately after the earthquake between November 27 and December 5, 1992, taking advantage of an already existing network measured by GPS in 1990 and 1991 (figure 1). We occupied a network of 13 points (figure 3), 6 located in the northern part of the Gulf and 7 in the

south, with three Ashtech PXII receivers. 12 points were already existing GPS marks, established during one or several previous campaigns:
- C, D, S, V, U, T, X, Y during our 1991 campaign (see Rigo et al. (1), this issue).
- A, C, D during our 1990 campaign.
- A, U, V, 31, 44, 62 during two greek-english campaigns in 1989 and 1991.

In general, the GPS data were collected during two daily sessions from 07:00 to 10:00 UTC and from 11:00 to 19:00 UTC. In this paper we deal only with the data collected at points of our 1991 GPS network and occupied at least twice : C, D, S, V, X, Y. We processed the data using the GAMIT software. We used the orbits transmitted by the satellites and the meteorological data measured in the field. The 1992 relative positions were then obtained from a three dimensional adjustment of the baselines. The RMS in this adjustment was 7mm, a value larger than the 3-4 mm average scatter on the baselines lengths found in 1991 (Rigo et al. (1), this issue). However, this RMS includes the vertical component, in general 3 times less accurate than the horizontal ones. Thus, we estimate that the horizontal accuracy of our 1992 network is 4-5mm; this value is in good agreement with the repeatability of the baselines measured two or three times in 1992 (Sbis-X : 0 mm, Sbis-D : 1 mm, Sbis-S : 6 mm, Sbis-V : 3 mm, X-Y : 1 mm). The accuracy on the displacement vectors presented hereafter is then expected to be in the 6-7 mm range, assuming a quadratic summation of the individual errors of each campaign.

To compare the two data sets, the adjusment of the 1992 data was done fixing one or several points at its 1991 position. Three different adjustments were done to check the stability of our solution:
- case 1: X fixed, all other free ("free" adjustment).
- case 2: X, D, Y fixed (i.e. southern coast fixed).
- case 3: D, Y fixed.

**Table** 2. Observed displacement of geodetic points under three different assumptions on the points supposed fixed at the two epochs. GAMIT software was used to process the GPS data.

| Point | Case 1 | | Case 2 | | Case 3 | |
|---|---|---|---|---|---|---|
| | dx (mm) | dy (mm) | dx (mm) | dy (mm) | dx (mm) | dy (mm) |
| C | 0 | 7 | -1 | 6 | -1 | 6 |
| D | 0 | 0 | fixed | | fixed | |
| S | -1 | 24 | 0 | 22 | 0 | 20 |
| V | -2 | 20 | -1 | 17 | -1 | 16 |
| X | fixed | | fixed | | 0 | -3 |
| Y | 1 | 5 | fixed | | fixed | |

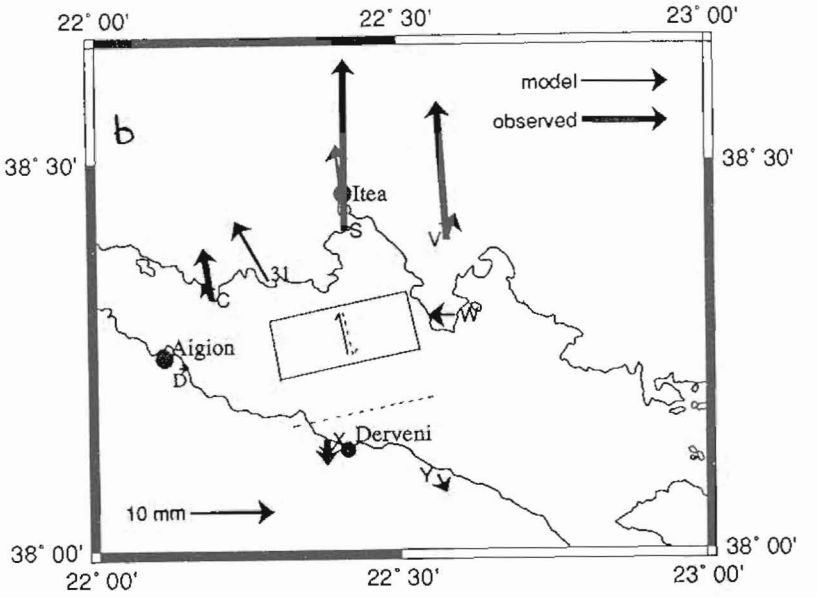


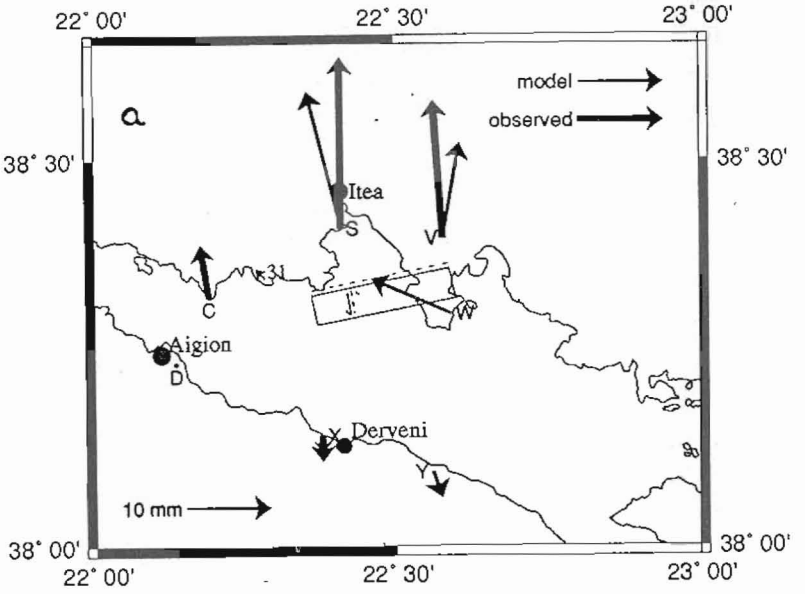


Fig.3. Observed (thick arrows) and predicted (thin arrows) displacements of the geodetic points, assuming a south dipping fault (3a) or a north dipping fault (3b). The corresponding dislocation plane is drawn in projection; the dashed line represents the intersection of this plane with the surface. Predicted displacements at points W and 31 are also plotted.

The displacement vectors in each case are summarized in table 2. The clearest feature in table 2 is the fact that the points S and V are displaced by ~20 mm to the north, almost independently of the choice of fixed points in the southern part of the Gulf. Then, it is possible to consider that the southern part of the Gulf remained relatively undeformed between the two campaigns with respect to the deformation that occurred across the Gulf itself. Moreover, the displacements of D and Y in case 1 demonstrate that there is no significant scale and orientation error in the comparison, so we conclude that the displacements found for S and V are significative both in amplitude and orientation. The displacement vectors used in our model (next section) are those calculated assuming D and Y fixed (table 2, case 3) and are presented in figure, 3.

In the following section, we present the model of dislocation used in this paper, and calculate our best solution in the two cases allowed by the focal mechanism: fault plane dipping north (low dip), fault plane dipping south (high dip).

## MODEL

To calculate the displacement vectors, we used a simple model of dislocation on a rectangle in an elastic half-space, following the formalism of Okada (1985). In this model, a fault is described by 9 parameters:

- location of the center of the upper edge of the fault (2 parameters)
- depth of this upper edge, width, length of the fault (3 parameters)
- strike and dip angles of fault plane (2 parameters)
- slip vector on fault plane: direction and amplitude (2 parameters)

These 9 parameters cannot be well resolved using only the geodetic data. Thus, using the focal mechanism (figure 2) discussed above we fixed three parameters: the strike and dip of fault plane and the slip direction. The number of remaining parameters is then 5. An additionnal constraint given by the body wave modeling is the value of the seismic moment Mo. This value is linked to the surface of faulting S and the amplitude of slip d by the relation Mo = mSd, with an uncertainty ranging usually between 30% and 50%. Because the fit with our geodetic data was better, we use in the following two dislocation models, a value of $6\ 10^{17}$ Nm for Mo, 15% larger than that deduced from seismicity, but in the range of the possible errors.

## FAULT PLANE DIPPING SOUTH

In this hypothesis, the fault plane has a relative high-dip ($60^{\circ}$) and the earthquake is supposed to have occurred on a fault antithetic to the main active faults that dip north (figure 1). We fixed the width of the fault at 8 km assuming that the upper bound was at 2 km depth (no surface breaks known, moderate damage), and that the lower bound was located at about 9 km depth, at the intersection with the north dipping discontinuity.

This geometry is inferred from the results of a seismicity study further west (Rigo et al. (2), this issue). We used an amplitude of 120 mm for the slip vector because we found that this value was relatively stable (between 100 and 130 mm) when the other remaining parameters (location of the fault and length) vary. The length of the fault (20 km) was simply deduced from the relation between the seismic moment, the surface of the fault and the displacement. Finally, we found the most probable location of the fault by inversion of the geodetic data. Table 3 shows the final parameters of our fault model and table 4 and figure 3a the corresponding observed and predicted displacements.

## FAULT PLANE DIPPING NORTH

Using the same procedure, we also tested models with the fault plane located on the main north-dipping structure. This type of models create displacements always lower than the south dipping models. The parameters of the north dipping model given in table 3 correspond to the model giving the largest displacements. The corresponding displacements are listed in table 4 and drawn in figure 3b.

Table 3. Parameters of the best fault model in the two hypothesis for the fault plane.

| | South-dipping fault | North-dipping fault |
|---|---|---|
| Location (center of the upper edge of the fault) | E 22°28'<br>N 38°18' | E 22°25'<br>N 38°14' |
| Length | 20 km | 20 km |
| Width | 8 km | 10 km |
| Upper limit | 2 km | 4 km |
| Slip amplitude | 120 mm | 100 mm |
| Dip-angle | 60° | 30° |
| Orientation of fault trace | N80E | N260E |

## DISCUSSION

The data and results presented above are not sufficient to choose between the two possible solutions for the fault plane (figure 4). The principal arguments for a fault plane located close to the north coast and dipping south are the following:
(a) the earthquake was felt much strongly along the northern coast of the Gulf than on the southern coast.
(b) the azimuth of the fault given by the focal mechanism is not in good agreement with the general orientation of the southern structures (figure 1).

(c) the displacements predicted with a fault plane dipping south are in better agreement with the observations than those predicted with a fault plane dipping north.

Table 4. Observed and predicted displacements in the two hypothesis for the fault plane

| | Observed | | Predicted (south-dipping fault) | | Predicted (north-dipping fault) | |
|---|---|---|---|---|---|---|
| Point | dx (mm) | dy (mm) | dx (mm) | dy (mm) | dx (mm) | dy (mm) |
| C | -1 | 6 | 0 | 0 | -1 | 2 |
| D | fixed | | 0 | 0 | 1 | 0 |
| S | 0 | 20 | -4 | 16 | -1 | 10 |
| V | -1 | 16 | 2 | 11 | 1 | 3 |
| X | 0 | -3 | 0 | -2 | 0 | -2 |
| Y | fixed | | 1 | -3 | 1 | -2 |
| W | not measured in 1992 | | -9 | 4 | -3 | 0 |
| 31 | 1991 data not yet available | | -1 | 1 | -4 | 7 |

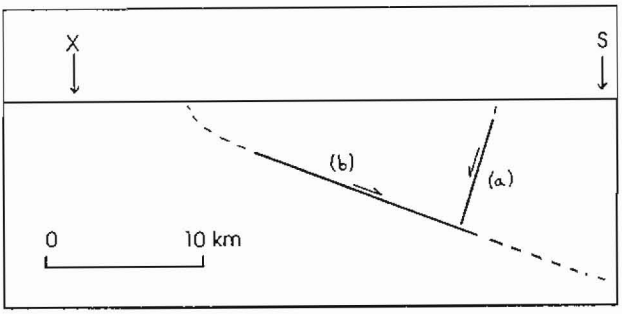


Fig.4. Cross section of the Gulf of Corinth at the longitude of points X and S. The two possible models for the earthquake (a and b) are plotted and refer to figure 3a and 3b.

Arguments (b) and (c) however should be discussed :
(b) : in the region of Derveni, the southern fault enters off shore with an azimuth compatible with the focal mechanism (figure 1)
(c) : although the observed displacements suggest a south dipping fault, this result was obtained neglecting the contribution of the continuous opening of the Gulf in the total deformation over the period 09/91-11/92. As none of our models for the earthquake predict displacements in C larger that 2 mm, we consider that the 6 mm displacement observed may be due to the continuous opening of the Gulf. The corresponding rate (5 mm/yr) is in relative good agreement with the rate deduced from the comparison of our measurements in 1990 and 1991 on the same line C-D : 8 mm/yr (10 mm/16 month). This value is lower than the value of 10 mm/yr obtained over 100 year by Billiris et al. (1991), and lower than the 15 mm/yr given by Rigo et al. (1) with data covering ~20 years. Although there is a discrepancy between the rate of 10-15

mm/yr found on long term data and the rate of 5-8 mm/yr found on our two series of measurements across the Gulf (1990-91 and 1991-92), it seems that this last value (5-8 mm/yr) represents the present opening across the Gulf (in the C, D area). Extrapolating this value in the X, S area may explain quite well the discrepancy between the observed displacements and those (lower) predicted by our preferred model. This conclusion is however speculative due to the small amount of displacements, close to the error bars, due to the small number of geodetic points, and due to the uncertainty on the seismic moment Mo. Further measurements on point W (displacement predicted : 11 mm, with an angle significantly different from that due to the continuous opening in the case of a north dipping fault) and analysis of the data of point 31 (no displacement expected from the earthquake on a south dipping fault, 8 mm in the case of north dipping fault, and some amount of displacement expected in both cases due to the continuous opening) should be extremely important to provide additional information on this earthquake.

## CONCLUSION

Two different and complementary techniques are used in this paper to characterize the earthquake ($M_s \sim 5.9$) that occured on 18/11/1992 in the Gulf of Corinth. The focal mechanism of the earthquake corresponds to pure normal faulting on a plane roughly oriented EW and dipping either north or south. Although our data are not sufficient to rule out definitively the hypothesis of a north dipping plane, we consider that the most probable hypothesis is that the earthquake occured on a plane dipping south, on a fault located close to the northern coast of the Gulf, antithetic to the main active faults. This solution is in better agreement with the geodetic data, and is more compatible with the fact that the earthquake was felt much strongly along the northern coast of the Gulf than along the southern coast. Moreover, even if the earthquake occured roughly at the same distance of the two coasts, more destructions should be expected in the south where the villages are built on recent marine terrasses than in the north where, except Itea, the villages are, in general, located on limestone.

Both hypothesis for the fault plane, predict displacements smaller than the observed values. This discrepancy is low in the case of a south-dipping fault (18 mm of extension predicted between X and S, 23 mm observed), a few mm higher in the case of a north-dipping fault (12 mm predicted), and may be explained in both cases by some amount of continuous opening of the Gulf in the total deformation. This continuous opening is found to range between 5 and 8 mm/yr as measured by us between points D and C on a 2.5 years period (5/90-11/92). Further measurements in point W and data processing for point 31 are expected to give more constraints on the 1992 earthquake and more information on the seismic and aseismic parts of the deformation in the short term (1990-1993) across the Gulf at the Derveni-Itea longitude. Our future GPS campaigns planned in this area, are also expected to allow a reexamination of our present results in a more general description of the superposition of seismic and aseismic

deformation in the Gulf of Corinth area.

ACKNOWLEDGMENTS

Stamatis Adonatos, Georges Lolos (NTU Athens) participated in the field campaign organized immediately after the earthquake. The GPS receivers used during this survey were borrowed by EDF (Electricité de France). This work is supported by the EEC contract EPOC-CT91-0043.

REFERENCES

Ambraseys,N.M. and Jackson,J.A., (1990). Seismicity and associated strain of central Greece between 1890 and 1988, Geophys. J. Int., 101, 663-708.

Billiris,H., Paradissis,D., Veis,G., England,P., Featherstone,W., Parsons,B., Cross,P., Rands,P., Rayson,M., Sellers,P., Ashkenazi,V., Davison,M., Jackson,J. and Ambraseys,N., (1991). Geodetic determination of tectonic deformation in Central Greece from 1900 to 1988, Nature, 350, 124-129.

Jackson,J.A., Gagnepain,J., Houseman,G. King,G.C.P., Papadimitriou,P., Soufleris,C. and Virieux,J., (1982). Normal faulting and geomorphological developpment of the Gulf of Corinth (Greece) : the Corinth earthquakes of February and March 1981, Earth and Planet. Sci. Let., 57, 377-397.

King,G.C.P., Ouyang,Z.X., Papadimitriou,P., Deschamps,A., Gagnepain,J., Houseman,G., Jackson,J.A., Soufleris,C. and Virieux,J., (1985). The evolution of the Gulf of Corinth (Greece): an afterskock study of the 1981 earthquakes, Geophy. J. R. Astr. Soc., 80, 677-693.

Mc Caffrey,R. and Abers,G., (1988). A program for inversion of teleseismic body waveforms on microcomputers, Air Force Geophysics Laboratory Technical Report AFGL - TR - 88-0099, Air Force Laboratory, Hanscom AFM, MA.

Liotier, (1989). Modélisation des ondes de volume des séismes de l'Arc Egéen, Rapport de DEA, Université Joseph Fourier de Grenoble 1, France, 99pp.

Nabelek,J., (1984). Determination of earthquake source parameters from inversion of body waves, PHD, Massachussets Institut of Technology, 360pp.

Okada,Y., (1985). Surface deformation due to shear and tensile faults in a half space, Bull. Seismol. Soc. Am., 75, 1135-1154.

Rigo,A., Briole,P., Lyon-Caen,H., Ruegg,J.C., Veis,G., Agatza-Balodimou,A.M., Mitsakiki,C., Papazissi,K. and Makropoulos,K., Deformation studies in the westren part of the Gulf of Corinth (Greece) : first results from GPS campaigns, accuracy and comparison with triangulation data, same issue (1).

Rigo,A., Lyon-Caen,H., Armijo,R., Bernard,P., Makropoulos,K., Papadimitriou,P., Deschamps,A. Fault plane solutions of microearthquakes and tectonic analysis in the western part of the Gulf of Corinth (Greece), same issue (2).